

# THE CALCULATION OF ELECTROWEAK RADIATIVE CORRECTIONS ON THE TOPONIUM RESONANCE\*

BY R. G. STUART

Max-Planck-Institut für Physik und Astrophysik, Werner-Heisenberg-Institut für Physik, P.O.Box 40 12 12,  
Munich, Fed. Rep. Germany

(Received September 28, 1987)

The methods used to calculate electroweak radiative corrections on the toponium resonance are discussed. Prospects for the measurement at LEP of these one-loop effects are examined.

PACS numbers: 12.15.Ii

This paper discusses the methods employed in the calculation of the electroweak radiative corrections to toponium. It is done in a very general manner with tedious specific details avoided as far as possible. It is hoped that in this way the general techniques which are of use in other contexts will be made clear. The work described here was the first calculation of the one-loop electroweak corrections in a bound system or a system where the fermion mass cannot be neglected. Contrary to naive expectation the bound state introduces a number of simplifications. For example it will be shown that the 3-point functions that occur can all be expressed as the sum of 2-point functions and similarly the 4-point functions are expressible in terms of 3-point functions. Much of what is presented here appears in Refs [1, 2].

Why look to toponium as laboratory to test the Glashow-Salam-Weinberg model at the one-loop level? It is by now well known that the best place to test the radiative corrections to the standard model is looking for deviations from predictions for the longitudinal polarization asymmetry in  $e^+e^- \rightarrow \mu^+\mu^-$ ,  $A_{RL}$ , on the  $Z^0$  resonance [3]. The polarization asymmetry is defined as,

$$A_{RL} = \frac{\sigma_R - \sigma_L}{\sigma_R + \sigma_L}, \quad (1)$$

where  $\sigma_{L(R)}$  is the production cross section for left (right) hand polarized beams. This however has its limitations. As a consequence of the  $Z^0$  exchange graph dominating the

---

\* Presented at the XXVII Cracow School of Theoretical Physics, Zakopane, Poland, June 3-15, 1987.

photon exchange, it turns out that the polarization asymmetry is largely independent of the outgoing fermion species. If polarized beams are not available, the forward-backward asymmetry,  $A_{FB}$ , can be examined but the relative sensitivity of the two quantities to radiative corrections is,

$$\delta A_{FB} = \frac{3}{2} A_{RL} \delta A_{RL}. \quad (2)$$

Thus  $\delta A_{FB}$  is considerably suppressed by the factor  $A_{RL}$  which is proportional to the charged lepton vector coupling to the  $Z^0$ . The polarization asymmetry for toponium production,  $e^+e^- \rightarrow V$ , is also the most favourable quantity (in the sense of being most sensitive to radiative corrections) available on that resonance. To identify the toponium state one can look for its characteristic decays such as the 3 gluon decay mode, identifiable by its three jet topology, and single quark decays characterised an isolated lepton, missing energy or aplanar event structure [4, 5] (In single quark decays, SQD, a single quark within the toponium decays). These modes have a sizeable branching ratio. The former exceeds 10% for  $m_t < 40$  GeV and the latter eventually dominates as  $m_t$  increases. When only unpolarized beams are available one can look at the forward-backward asymmetry for muon pairs given by,

$$A_{FB} = \frac{4}{3} \frac{N_F - N_B}{N_F + N_B}. \quad (3)$$

$N_{F(B)}$  is the number of muons emitted in the forward (backward) direction. This is related to polarization asymmetry for muon pairs by [6, 7]

$$A_{FB} = A_{RL}^2 \quad (4)$$

in lowest order but including beamsread effects. Note, however, that  $A_{RL}$  is here not so small as on the  $Z^0$  resonance so that the sensitivity of  $A_{FB}$  is less suppressed. Of course, for both of these, interference with the continuum must be considered but for  $M_Z$  well separated from the toponium mass,  $M_V$ , it is smaller than the corrections. Final state radiation also modifies  $A_{FB}$  since muons can be bremsstrahlunged (apologies to German colleagues) into the 'wrong' hemisphere. A Monte Carlo generator is required to take account of this. Since parity is not conserved in weak interactions, the toponium state is produced with some preferred polarization. The expectation value of the polarization is directly measured by the muon asymmetry in SQD's,

$$\langle S_z \rangle = \frac{1}{f} \frac{N_F - N_B}{N_F + N_B}, \quad (5)$$

$f$  denotes the analysing power of the leptons and in a simple model it is given by 3/8 [5]. Note also that  $\langle S_z \rangle$  is also related to the polarization asymmetry for muon pairs in (4) by,  $\langle S_z \rangle = A_{RL}$ .

Experimental prospects for precision measurements of these quantities are quite sensitive to the exact value of the toponium mass. In a recent study [4] it was assumed that the toponium mass lies in the range 60–110 GeV and that the integrated luminosity is 80–100 pb<sup>-1</sup> which corresponds to 80 days of running at LEP. With unpolarized beams,

$A_{\text{RL}}$  could be measured through SQD's to 0.05. When polarized beams are available this figure drops to 0.02. There exists a possibility that the beams spread could be further reduced [8] or that the running time could be prolonged. The large beams spread at SLC seems to preclude precision measurements on toponium.

We now turn to the theoretical side of the calculation. The Euclidean metric is used throughout so that  $p^2$  is negative for time-like momenta. Fig. 1 shows a general production

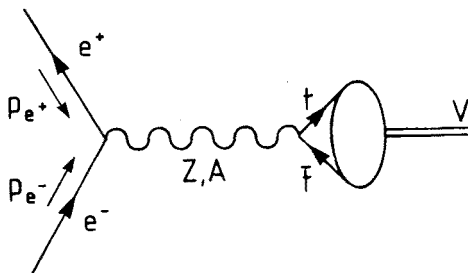


Fig. 1. The lowest order diagrams for  $e^+e^- \rightarrow V$ . The lens shaped blob converts open  $t\bar{t}$  into bound toponium

diagram for toponium,  $e^+e^- \rightarrow V$ . The lens shaped blob may be thought of as a vertex that converts open  $t\bar{t}$  to the bound toponium system. A prescription for calculating with bound states is given by [9]. It will not be rederived here but an attempt will be made to justify the prescription in a general way. The effective vertex in Fig. 1 could be expected to have the form,  $C\gamma_\mu\delta^4(p-p')$  for some constant  $C$  and internal quark momenta  $p, p'$ . The  $\gamma_\mu$  arises because we are chiefly concerned here with the lowest lying  $^3S_1$  vector resonance. Axial vector resonances are less important because their couplings depend on the derivative of the quark wave function at the origin. This is closely related to  $v/c$  for the internal quarks. The  $\delta$ -function appears since toponium is a weakly bound nonrelativistic system requiring that the internal quarks be at rest with respect to one and other. Later it will be seen that this fact is responsible for substantial simplifications in the loop calculations. Since the top quarks are bound through a point-like interaction, the constant,  $C$  should depend on the wave function at the origin,  $R(0)$ . The bound state prescription in the case of production is that for an operator  $\mathcal{O}$ , whose effect on free quarks would be given by  $\bar{v}\mathcal{O}u$ , then,

$$\bar{v}\mathcal{O}u \Rightarrow \frac{f_V M_V}{4} \text{Tr} [\mathcal{O}(-i\not{P} + M_V)\gamma_\mu] E_\mu, \quad (6)$$

where,

$$P^2 = -M_V^2,$$

$$M_V^2 = \text{the toponium mass},$$

$$E_\mu = \text{the toponium polarization},$$

$$f_V = R(0)/\sqrt{\pi M_V^3}.$$

The form is not surprising. Again since toponium is weakly bound the internal quarks may be regarded as being on-shell and replacing the external states by propagators sandwiching the operator  $\mathcal{O}$  we get at once,

$$\bar{v}\mathcal{O}u \Rightarrow C' \text{Tr} \left[ \mathcal{O} \left( -i \frac{\not{P}}{2} + \frac{M_V}{2} \right) \gamma_\mu \left( i \frac{\not{P}}{2} + \frac{M_V}{2} \right) \right]. \quad (7)$$

Anticommuting the  $i\not{P} + M_V$  through  $\gamma_\mu$  and dropping the term containing  $p_\mu$  since  $E \cdot p = 0$  yields the form above. Fig. 2 shows the complete set of one-loop corrections that must be considered. Other one-loop corrections that affect the Z and photon propagators or the  $e^-Z e^+$  and  $e^-A e^+$  vertex have been calculated elsewhere [10, 11]. Here  $\phi_Z$  and  $\phi_W$  are Goldstone bosons associated with the Z and W respectively, and H is the physical Higgs. Note in particular that the Higgs enters in Fig. 2d and i. The diagram in Fig. 2i however is found to contribute in the same way to both photon and Z exchange and therefore cancels out in asymmetries. The diagram of Fig. 2d is then the sole source of Higgs dependence apart from that occurring as corrections to the Z and photon propagators and implicit

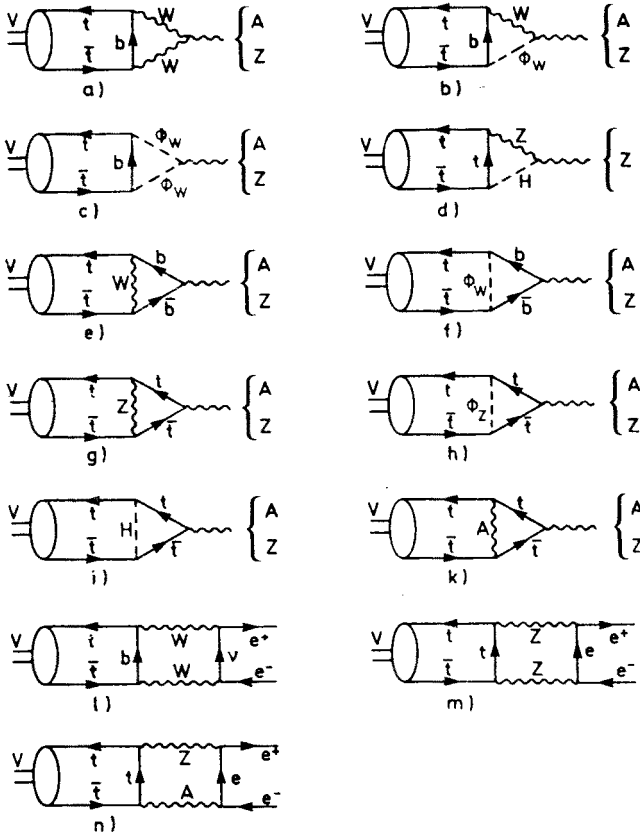


Fig. 2. Feynman diagrams relevant for the evaluation of one loop corrections. Permutations have been omitted

in the calculated value of  $\sin^2 \theta_w$ . Such contributions can be tested already in  $e^+e^- \rightarrow \mu^+\mu^-$ . Fig. 2k also does not contribute to the asymmetry.

Let us consider a particular example of the loop graphs. Take Fig. 2a. After applying Feynman rules in the usual way and applying the prescription of (6) an expression proportional to,

$$\int \frac{d^n q}{i\pi^2} \frac{F_0 \delta_{\mu\nu} + F_1 q_\mu q_\nu + F_2 P_\mu q_\nu + F_3 q_\mu P_\nu}{[q^2 - i\varepsilon] [(q - \frac{3}{2}P)^2 + M_W^2 - i\varepsilon] [(q + \frac{3}{2}P)^2 + M_W^2 - i\varepsilon]} \quad (8)$$

is obtained. Here the use of dimensional regularization is signalled by the differential  $d^n q$  where  $n$  is the (complex) dimensionality of space-time. For further details see Ref. [12]. Note that since the light quark masses are neglected there is only one 'free' momentum,  $P$ , in the problem and even then  $P^2 + M_V^2 = 0$  on the resonance. In the integral (8) the terms proportional to  $F_2 P_\mu q_\nu + F_3 q_\mu P_\nu$  are dropped immediately since they will be contracted with the (conserved) current of the massless electron. The remaining terms integrate up to,

$$F_0 \delta_{\mu\nu} + F_1 q_\mu q_\nu \rightarrow G_0 \delta_{\mu\nu} + G_1 P_\mu P_\nu. \quad (9)$$

The second term is dropped for the reasons just described. It is possible to extract the coefficient  $G_0$  directly from the integral (8) expressed as a scalar integral by means of the projection operator,

$$\frac{1}{n-1} \left( \delta_{\mu\nu} - \frac{P_\mu P_\nu}{P^2} \right). \quad (10)$$

Here  $n$  is again the dimensionality of space-time and  $\gamma_\mu \gamma_\mu = n$ . The integrals that are obtained in the vertex corrections (Figs. 2a-k) are in general divergent and ' $n$ ' must be explicitly kept in order to properly account for this. In dimensional regularization logarithmically divergent quantities appear as

$$\begin{aligned} \Delta &= \pi^{\frac{n}{2}-2} \Gamma\left(2 - \frac{n}{2}\right) \\ &\xrightarrow{n \rightarrow 4} \frac{1}{2 - \frac{n}{2}} - \gamma - \ln \pi. \end{aligned} \quad (11)$$

$\gamma = 0.5772\dots$  is Euler's constant. Note in particular that as  $n \rightarrow 4$ ,  $n\Delta \rightarrow 4\Delta - 2$  not  $4\Delta$ . After projection,

$$F_0 \delta_{\mu\nu} + F_1 q_\mu q_\nu \rightarrow \left[ F_0 + \frac{P^2 q^2 - (P \cdot q)^2}{(n-1)P^2} F_1 \right] \delta_{\mu\nu} + G_1 P_\mu P_\nu. \quad (12)$$

It can be checked rigorously that projection and integration are commuting operations. Thus a three denominator integral (3-point function) is obtained with no free Lorentz indices. Passarino and Veltman [13] have shown how to reduce such an integral to the

sum of two denominator integrals (2-point functions) plus one three denominator integral with a '1' in its numerator. In the present case things are even simpler as the 3-point function is absent. We now investigate the conditions under which this final simplification can occur. Take a general scalar 3-point function,

$$C_0(p_1, p_2; m_1, m_2, m_3) = \int \frac{d^n q}{i\pi^2} \frac{1}{[q^2 + m_1^2 - i\epsilon][(q + p_1)^2 + m_2^2 - i\epsilon][(q + p_1 + p_2)^2 + m_3^2 - i\epsilon]}. \quad (13)$$

For it to reduce to 2-point functions it is enough that the numerator is expressible as a linear combination of the factors in the denominator and hence that,

$$\begin{vmatrix} 1 & 1 & 1 \\ 0 & p_1^2 & p_1^2 + p_1 \cdot p_2 \\ 0 & p_1 \cdot p_2 & p_1 \cdot p_2 + p_2^2 \end{vmatrix} = p_1^2 p_2^2 - (p_1 \cdot p_2)^2 = 0. \quad (14)$$

For a general vertex with incoming momenta,  $p_1$ ,  $p_2$  and  $p_3$  it is simple to show that,

$$p_1^2 p_2^2 - (p_1 \cdot p_2)^2 = p_1^2 p_3^2 - (p_1 \cdot p_3)^2 = p_2^2 p_3^2 - (p_2 \cdot p_3)^2. \quad (15)$$

If one of the particles has time-like momentum (as in the present case) we can boost to that particle's rest frame and show that all the particles are relatively at rest. This is precisely the condition realized by the  $\delta$ -function in the effective vertex in the description of the bound state formalism.

The vertex diagrams just calculated are divergent. Their divergences are cancelled by a counterterm contribution. This goes through in much the same way as for light fermions, see Ref. [10], but with one qualification. The counterterm is obtained from fermion wave function renormalization and involves the graphs shown in Fig. 3. A sufficiently heavy top quark may decay into a W boson and a b-quark and so the graphs containing a virtual W or  $\phi_w$  develop an imaginary part for  $m_t > M_w$ . However counterterms must be real otherwise they would lead to a violation of unitarity. Careful treatment is needed but it transpires that the imaginary part only contributes as an  $O(\alpha^2)$  correction and does not give trouble in the order of interest.

Turn now to the box diagrams shown in Fig. 21–n. By simple power counting they can be seen to all be finite. Moreover, since toponium is a neutral state, soft photons decouple from it and there are no infrared divergences in the Z–A box diagram of Fig. 2n. The magnitude of the contributions from the three types of box is governed by two competing effects, combinatoric factors and factors of  $\sin^2 \theta_w$ . The Z–A, Z–Z and W–W boxes have combinatoric factors 4, 2, and 1 respectively but are suppressed by relative factors,  $\sin^4 \theta_w$ ,  $\sin^2 \theta_w$  and 1 by the coupling which finally dominates. It is therefore the W–W box diagram which gives the largest effect. In calculating the boxes we can play the same game as for the vertices and project out the part proportional to  $\delta_{\mu\nu}$  by means of the operator,

$$\frac{1}{2} \left( \delta_{\mu\nu} - \frac{P_\mu P_\nu}{P^2} - \frac{l_\mu l_\nu}{l^2} \right), \quad (16)$$

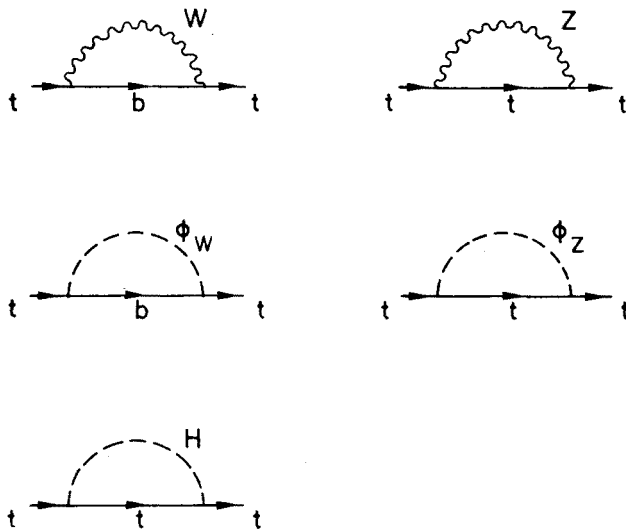


Fig. 3. The Feynman diagrams involved in top quark wave function renormalization. The diagrams containing a virtual  $W$  boson or  $\phi_W$  develop an imaginary part for  $m_t > M_W$  ( $m_b = 0$ )

where for incoming electron momentum,  $p_{e-}$ , and positron momentum,  $p_{e+}$ ,

$$P = p_{e-} + p_{e+} \quad l = (p_{e-} - p_{e+})/2. \quad (17)$$

The integrals depend only on  $P^2$  since  $l^2 = -P^2/4$  and  $P \cdot l = 0$ . There is no need to keep the  $n$  of dimensional regularization in (16) because the integrals do not diverge. Also in this case it is found that the 4-point scalar integrals thus obtained reduce to 3-point functions. Explicit expressions for the box diagrams can be found in Ref. [2]. The 3-point integrals just have to be evaluated. The general  $C_0$  in (13) can be written after Feynman parametrization as,

$$C_0(p_1, p_2; m_1, m_2, m_3) = \int_0^1 dx \int_0^x dy [ax^2 + by^2 + cxy + dx + ey + f]^{-1}, \quad (18)$$

with,

$$\begin{aligned} a &= -p_2^2, & b &= -p_1^2, & c &= p_1^2 + p_2^2 - p_3^2, \\ d &= m_2^2 - m_3^2 + p_2^2, & e &= m_1^2 - m_2^2 + p_1^2 - p_2^2, & f &= m_3^2 - i\varepsilon. \end{aligned}$$

Recall that  $p_3 = -p_1 - p_2$ . If  $m_3 = 0$ , as can be arranged for all integrals of interest here, we make the substitution  $x \rightarrow xy$  and get,

$$C_0 = \int_0^1 dy \frac{1}{by^2 + cy + a} \{ \ln [by^2 + (c+e)y + (a+d) - i\varepsilon] - \ln [ey + d - i\varepsilon] \}. \quad (19)$$

Note that the integrand has zero residue at the pole and is therefore independent of the exact contour of integration. A general expression for (19) in terms of Spence (dilogarithm) functions,

$$\text{Sp } x = - \int_0^x \frac{\ln(1-t)}{t} dt \quad (20)$$

is known, see Ref. [14], but the task of reducing the number of Spence functions in the final answer to a minimum remains something of an art. Two important relations, valid for complex  $x$  and  $y$ , of use in this connection are,

$$\text{Sp } x + \text{Sp } (-x) = \frac{1}{2} \text{Sp } x^2, \quad (21)$$

$$\text{Sp} \left( \frac{1}{x} \right) + \text{Sp} \left( \frac{1}{y} \right) = -\frac{1}{2} \ln^2 \left( -\frac{x}{y} \right), \quad x+y=1 \quad (22)$$

and the generalization of Hill's formula for complex arguments,

$$\begin{aligned} \text{Sp } xy &= \text{Sp } x + \text{Sp } y + \text{Sp} \frac{xy-x}{1-x} + \text{Sp} \frac{xy-y}{1-y} \\ &+ \frac{1}{2} \left[ \ln \frac{1-x}{1-xy} + \ln \frac{1-y}{1-xy} \right]^2 \\ &+ \eta \left( \frac{1}{1-x}, 1-xy \right) \ln x + \eta \left( \frac{1}{1-y}, 1-xy \right) \ln y, \end{aligned} \quad (23)$$

where  $\eta(x, y) = \ln xy - \ln x - \ln y = 0, \pm 2\pi i$  but does not in general vanish for complex  $x$  and  $y$ .

In this calculation one finds for  $u = M_Z^2/M_V^2$ ,

$$M_V^2 C_0(\tfrac{1}{2}P+l, -P; 0, M_Z, M_Z) = -\ln^2 \left( \frac{\sqrt{1-4u}+1}{\sqrt{1-4u}-1} - i\epsilon \right), \quad (24)$$

$$M_V^2 C_0(l, \tfrac{1}{2}P-l; 0, 0, M_Z) = 2 \left[ \frac{\pi^2}{4} - \text{Sp} \left( 1 - \frac{1}{2u} \right) + \text{Sp} \left( \frac{1}{2u} - 1 + i\epsilon \right) \right], \quad (25)$$

$$M_V^2 C_0(l, \tfrac{1}{2}P; 0, \tfrac{1}{2}M_V, M_Z) = \frac{\pi^2}{6} - \text{Sp} \left( 1 - \frac{1}{u} \right). \quad (26)$$

The expression for the Z-A box possesses a logarithmic divergence as  $M_V \rightarrow M_Z$ . This can be regulated by incorporating the toponium binding energy,  $E_b$ , and the  $Z^0$  decay width,  $\Gamma_Z$ , into the results.

So far no attention has been paid to QED and QCD corrections. Since toponium is neutral, final state radiation can be ignored. Initial state bremsstrahlung is constrained to be very soft since the toponium width is small and the emission of a hard photon will



shift off the resonance. Its effect therefore is as an overall factor which cancels in asymmetries. QCD corrections can be safely ignored to  $O(\alpha)$ . The correction of order  $\alpha_s$  affects only the overall normalization. Corrections of order  $\alpha\alpha_s$  arise from two distinct sources. Some originate from QCD corrections at the toponium vertex together with electroweak corrections at the electron vertex or to the boson propagators. These again essentially go into the normalization. The other source is simultaneous QCD and electroweak corrections at the toponium vertex. They are not enhanced by large logarithms and thus are truly of order  $\alpha_s/\pi$  relative to those evaluated here.

The course of the calculation in practice runs as follows. The values of  $\alpha$ ,  $M_Z$  and  $G_\mu$  (the muon decay constant) are taken from data since they will be the most precisely measured quantities at the time toponium measurements start. The value of  $\sin^2 \theta_W$  (and hence  $M_W$ ) consistent with these data is then calculated using formulas due to Sirlin [15] accurate to  $O(\alpha)$  plus leading logarithms from higher orders. The result will depend on the assumed value for the Higgs mass and also on the top quark mass. The value obtained is then used in the calculation of all further loop corrections. Since there is no physics that is unique to the toponium system in the calculation of  $\sin^2 \theta_W$  we define the lowest order asymmetry

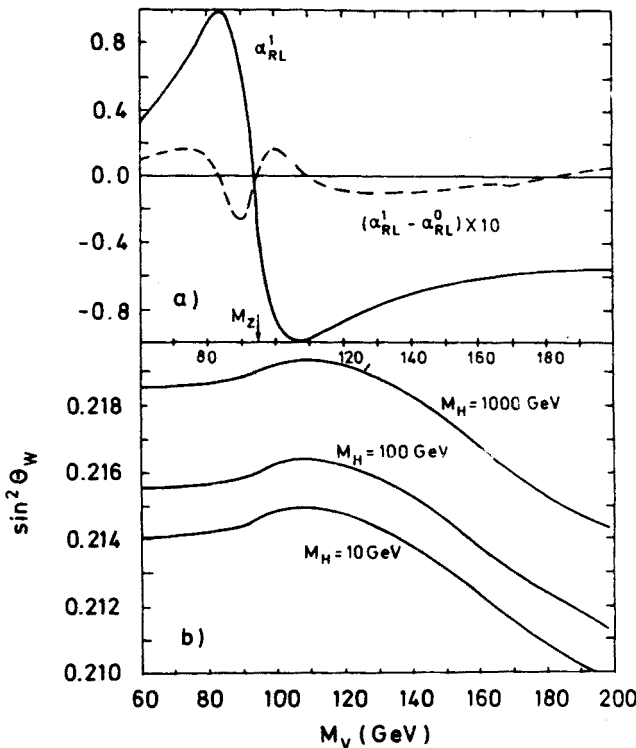


Fig. 4. a) Prediction for the polarization asymmetry as a function of the toponium mass for  $M_H = 100$  GeV and  $M_Z = 94$  GeV. Solid line: Full one loop correction. Dashed line: difference between first order and lowest order prediction; b) Value of  $\sin^2 \theta_W$  used both for lowest order and one loop corrected prediction for different values of  $M_H$

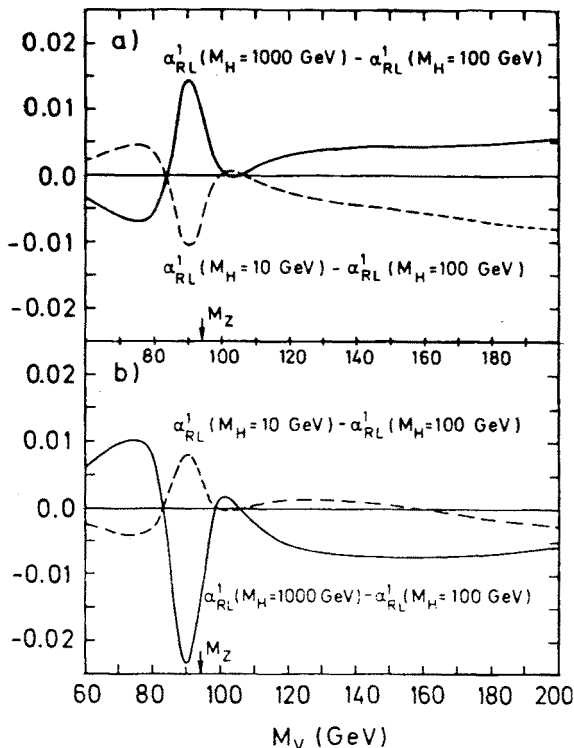


Fig. 5. Change in the asymmetry  $\alpha_{RL}(M_H) - \alpha_{RL}(100 \text{ GeV})$  for a Higgs mass of 1000 GeV (solid line) and 10 GeV (dashed line), a) including the variation of the Weinberg angle, b) fixing the Weinberg angle to the value calculated for  $M_H = 100 \text{ GeV}$

to be the asymmetry obtained from tree graphs for the asymmetry, Fig. 1, but with the calculated value of  $\sin^2 \theta_w$ . The first order corrected asymmetry is the asymmetry with *all* corrections included. This asymmetry along with its difference from the lowest order asymmetry is displayed in Fig. 4a. The difference is free from universal and large logarithmic corrections from  $\sin^2 \theta_w$  and we are left with the purely electroweak corrections that are of real interest. The variation of the calculated value of  $\sin^2 \theta_w$  with  $M_H$  and  $M_V$  is shown in Fig. 4b.

Unfortunately the contribution of the diagram in Fig. 2d, which was the only place we might hope to have seen effects from the coupling between the Higgs and a fermion, is at most 0.001 for  $M_V < 160 \text{ GeV}$ . The Higgs once again eludes us. There remain however loop diagrams in the Z propagator which contain the Higgs and as mentioned previously there is dependence in  $\sin^2 \theta_w$  on  $M_H$ . In Fig. 5a the two effects are plotted together and in Fig. 5b with a fixed value for  $\sin^2 \theta_w$ . The difference between extreme choices of the Higgs mass may be up to 0.025.

The size of the box diagrams is illustrated in Fig. 6. The change in the asymmetry is shown when the W-W and Z-A box diagrams are dropped. The Z-Z box contributes less than 0.001. Note that in the high mass region the W-W box contribution would be

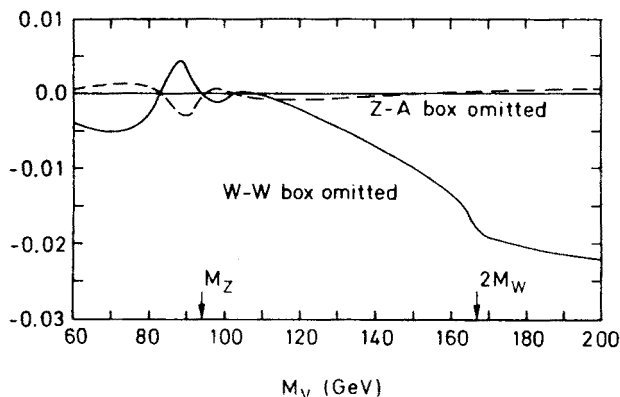


Fig. 6. Change in the asymmetry if the W–W or the Z–A box diagram is dropped. The corresponding change for the Z–Z box is below 0.001

just observable by itself but it conspires with the other corrections in such a way that the overall correction is substantially smaller. This type of thing happens in many other cases and one might speculate about a ‘Law of Cussardness’ for radiative corrections.

To conclude then we see that the effects of electroweak radiative corrections to toponium are small but may just be observable at LEP if polarized beams are available. However the Higgs-fermion coupling escapes detection.

## REFERENCES

- [1] B. Grzadkowski, P. Krawczyk, J. H. Kühn, R. G. Stuart, *Phys. Lett.* **163B**, 247 (1985); B. Grzadkowski, P. Krawczyk, J. H. Kühn, R. G. Stuart, *Phys. Lett.* **176B**, 456 (1986).
- [2] B. Grzadkowski, P. Krawczyk, J. H. Kühn, R. G. Stuart, *Nucl. Phys.* **B281**, 18 (1987).
- [3] B. W. Lynn, R. G. Stuart, *Nucl. Phys.* **B253**, 216 (1985); B. W. Lynn, M. E. Peskin, R. G. Stuart, in: *Physics at LEP*, CERN 86-02, eds. J. Ellis, R. Peccei, 1986, p. 90.
- [4] LEP Study Group, W. Buchmüller et al., *Toponium Physics at LEP*, in *Physics at LEP*, CERN 86-02, eds. J. Ellis, R. Peccei, 1986, p. 203.
- [5] J. H. Kühn, K. H. Streng, *Nucl. Phys.* **B198**, 71 (1982).
- [6] A. Martin, unpublished.
- [7] S. Güsken, J. H. Kühn, P. Zerwas, *Nucl. Phys.* **B262**, 393 (1985) and references therein.
- [8] J. M. Jowett, preprints CERN LEP TH 85-04 (1985), CERN LEP Note 544 (1985).
- [9] J. H. Kühn, J. Kaplan, E. G. O. Safiani, *Nucl. Phys.* **B157**, 125 (1979).
- [10] R. G. Stuart, Oxford University, D. Phil. Thesis (1985); Rutherford and Appleton Lab. Report, RAL T 008.
- [11] M. Böhm, W. Hollik, H. Spiesberger, *Fortschr. Phys.* **34**, 687 (1987).
- [12] G. 't Hooft, M. Veltman, *Diagrammar*, in *Particle Interactions at Very High Energies*, eds. D. Speiser, F. Halzin, J. Weyers, Plenum, New York.
- [13] G. Passarino, M. Veltman, *Nucl. Phys.* **B160**, 151 (1979).
- [14] G. 't Hooft, M. Veltman, *Nucl. Phys.* **B153**, 365 (1979).
- [15] A. Sirlin, *Phys. Rev.* **D22**, 93 (1980); *Phys. Rev.* **D29**, 89 (1984).